



Cite this: DOI: 10.1039/c4ta03889d

Tailored design of palladium species grafted on an amino functionalized organozinc coordination polymer as a highly pertinent heterogeneous catalyst†

H. Choudhary, S. Nishimura and K. Ebitani*

The design of a highly active and stable heterogeneous palladium catalyst is gaining a lot of attention because of its increasing importance in the organic syntheses of commodity chemicals. Herein, we report the tailored synthesis of palladium species grafted on a highly stable amino functionalized organozinc coordination polymer (denoted as Pd/AZC) and its extraordinary catalytic performances in the Suzuki–Miyaura coupling (SMC) reaction. It achieved the highest turnover number of 2 106 720 (>99% yield) in air among the most reported palladium catalysts for the SMC reaction of bromobenzene. The as-prepared Pd/AZC composite is also successfully applied for the catalysis of Mizoroki–Heck coupling, hydrogenation of nitro, and $-C\equiv C-$ functional groups. Since the developed AZC support has thermal stability at least up to 573 K, it possesses high potential for grafting various metal species as catalytically active centers for a wide range of metal-catalyzed reactions.

Received 28th July 2014
Accepted 7th September 2014

DOI: 10.1039/c4ta03889d

www.rsc.org/MaterialsA

1. Introduction

In recent decades, porous coordination polymers (PCPs) have been an area of interest in many fields, namely energy, catalysis and separation. PCPs are inorganic–organic hybrid advanced materials with metal ions as the inorganic center and organic ligands as the linker with well-defined channels/pores. The prime reason of increasing attention on the PCP materials lies in the ease of tuning their structural features and relative properties for wide-range potential applications.^{1–3} For instance in terms of catalytic performances, because of this tunability, their structures can be precisely controlled to similarly incorporate active catalytic centers (in channels/pores) as enzymes which are extremely active and selective catalysts owing to the architectural active pockets in well-defined cavities.

Organic transformations such as C–Z (Z = C, O, N, *etc.*) coupling, hydrogenation, and oxidation have found potential industrial applications using transition metals (such as Au, Pd, Pt, *etc.*) catalysts. Among these, the Suzuki–Miyaura coupling (SMC) reaction using the Pd catalyst^{4–7} has become more like a ritual for the regioselective formation of C–C bonds in modern organic chemistry.^{8–13} Because of the tolerance of the SMC reaction for a wide range of substrates under milder conditions

in the presence of readily available organoboronic acids, the SMC reaction has been extensively employed as a handy methodology in the syntheses of natural products, pharmaceuticals and supra-molecular assemblies throughout the globe.^{8–13} The homogeneous Pd catalytic processes have higher activity and selectivity than their heterogeneous counterparts; however, they have serious issues of recovery and reusability. The reasons for the limited activity of the heterogeneous catalyst might be the poor accessibility of reactants to the active sites and/or fast deactivation by agglomeration of unstable Pd species into inactive Pd particles. Thus, designing a highly active and stable, heterogeneous Pd catalyst constitutes one of the important objectives for the transition metal-catalyzed SMC reaction and other catalytic reactions.^{14,15}

We successfully fabricated such a coordination polymer to graft drastically low palladium using a ligand design methodology. Herein, we present the synthesis, catalysis and structural characterization of a monomeric palladium species grafted on an amino functionalized organozinc coordination polymer (denoted as Pd/AZC) as a highly active and easily reusable heterogeneous catalyst for the SMC reaction with a high turnover number (TON). Recently, Deraedt and Astruc compiled a report on Pd nanoparticles (both homogeneous and heterogeneous) for the cross coupling reaction with concluding remarks on forthcoming challenges of both stabilization and improvement of catalytic efficiency.¹⁶ Various researchers have reported TON in the range of 100–3 500 000 for haloarenes (the average TON being 85 000 for bromobenzene) by homogeneous and heterogeneous catalyses.^{17–30} Different supports such as

School of Materials Science, Japan Advanced Institute of Science and Technology, 1-1 Asahidai, Nomi, Ishikawa 923 1292, Japan. E-mail: ebitani@jaist.ac.jp

† Electronic supplementary information (ESI) available: Catalytic activity optimization, reusability graph, detailed characterization of AZC (XAFS, XPS, IR and XRD), proposed mechanism, and NMR & MS of organic compounds. See DOI: 10.1039/c4ta03889d

activated carbon or carbon nanotubes,^{31–34} metal organic frameworks,^{21,29,35,36} zeolites,^{23,37–39} and mesoporous silica^{25,40–42} have been utilized for the SMC reaction.^{43–45} The activities were observed as a function of easy access of the substrates and reagents to active species. Okumura *et al.* demonstrated that the Pd/USY catalyst can give a TON of 13 000 000 using bromobenzene as the substrate only under a H₂ atmosphere without commenting on catalyst reusability.²³

In this contribution, we designed an organozinc coordination polymer with amino functionality for efficient grafting of Pd species leading to highly dispersed and easily accessible active centers. Because such PCPs have a regular microporous structure and a significant high surface area,^{1–3} the synthesized organometallic coordination polymer is believed to possess a highly porous structure that facilitates the access of substrates to the firmly held active Pd species with amino moieties. The catalytic system described here is supposed to be a promising synthetic protocol for the development of advanced metal-supported catalysts because of the following advantages: (i) high catalytic activity and selectivity under an air atmosphere, (ii) easy recovery and high reusability, and (iii) restricted homocoupling of phenyl boronic acid in the Pd-catalyzed SMC reaction.

2. Experimental

2.1 Materials

Phenylboronic acid, palladium chloride, zinc nitrate hexahydrate (Zn(NO₃)₂·6H₂O), toluene, methyl isobutyl ketone, benzyl alcohol, benzaldehyde, nitrobenzene, aniline, cinnamaldehyde, 3-phenylpropionaldehyde and standard solutions (1000 ppm) of palladium and zinc were purchased from Wako Pure Chemical Industries, Ltd. Potassium chloride, potassium carbonate (K₂CO₃), lithium carbonate, cesium carbonate, calcium carbonate, styrene, dimethylsulfoxide, acetone, *N,N*-dimethylformamide (DMF), methanol, acetonitrile, ethanol, *N,N*-dimethylacetamide, zinc oxide, succinic acid and sodium hydroxide were procured from Kanto Chemical Co., Inc. Tokyo Chemical Industry Co., Ltd. supplied bromobenzene, maleic anhydride and naphthalene whereas chlorobenzene was bought from Junsei Chemical Co., Ltd. QuadraPure® TU, 1-methyl-2-pyrrolidinone, 2-aminoterephthalic acid (ATA), tetrabutylammonium bromide (TBAB), stilbene, 1,1-diphenylethylene and zinc acetate (Zn(OAc)₂) were obtained from Sigma-Aldrich, Co. LLC.

2.2 Strategy for catalyst design

In general, the inclusion of facile access to the active species and firm binding of the supported active species have proved as an extra advantage to the heterogeneous catalyst. We really desired to fabricate such a heterogeneous material for the SMC reaction with features to hold the easily accessible active Pd firmly. The PCPs could be synthesized by controlled stitching of organic molecules with inorganic molecules especially the transition metals fascinated us. In principle, the Pd–N bonds are relatively strong, and thus we craved to choose an organic

moiety with a nitrogen containing functional group such as an amine, and thereby we selected 2-aminoterephthalic acid (ATA) as the organic linker for PCP. While zinc as the metal center was selected owing to its relative abundance, low cost and significant catalytic characteristics. The obtained amino functionalized organozinc coordination polymer (AZC) may facilitate to hold active Pd species with high dispersibility derived from amino functionality and the porous framework of PCP compounds.

2.3 Catalyst synthesis

2.3.1 Synthesis of the amino-functionalized organozinc coordination polymer (AZC). ATA (5 mmol) and Zn(NO₃)₂·6H₂O (5 mmol) in DMF (35 mL) were sealed in a 100 mL Teflon lined autoclave, and heated to 413 K (heating rate; 4 K min^{−1}) in a programmable oven and maintained at the same temperature for 24 h. The synthesis method involved the use of DMF as the solvent which slowly dissociates at higher temperature to deprotonate ATA, which in turn reacts with Zn(NO₃)₂·6H₂O to form the organozinc coordination polymer. The oven was allowed to cool to room temperature slowly. The solid residue obtained was filtered and washed with a small amount of DMF. Brownish blocks were obtained and dried *in vacuo* before grinding them to afford a light brown powder in a pestle mortar. These dried brown powders were further treated with ethanol at 353 K for 24 h in order to remove DMF and filtered and dried *in vacuo* to obtain “AZC”. Elemental analysis (%) for prepared AZC was found as C, 37.2; H, 2.0; N, 6.2; Zn, 27.3. To account for the result, a molecular formula was suggested Zn₄(ATA)₃(NO₃)₂ (or C₂₄H₁₅N₅O₁₈Zn₄): C, 31.2; H, 1.6; N, 7.6; Zn, 28.4.

2.3.2 Synthesis of the palladium grafted amino-functionalized organozinc coordination polymer (Pd/AZC). About 0.5 g of palladium chloride with 0.5 g potassium chloride were weighed and suspended in 50 mL water. The solution was sonicated with occasional stirring for 30 minutes to obtain a homogeneous palladium stock solution with a concentration of about 10 mg of PdCl₂ per mL of the stock solution. In a typical synthesis of 0.5 wt% Pd/AZC, a calculated amount of solution (208 μL, if the concentration of stock solution is 10 mg PdCl₂ per mL) was taken in a round bottomed flask and 15 mL of water was added. To this solution, 250 mg AZC was added and stirred at room temperature for 6 h, and then at 353 K for 14 h. The obtained brown colored solution was filtered, washed with about 1 L of water and dried *in vacuo* at room temperature. The dried powder was ground to obtain Pd/AZC (238 mg). Various palladium grafted AZC catalysts were denoted as xPd/AZC; where the x is Pd content on support as (wt/wt) in theory.

2.4 Catalytic testing for the Suzuki–Miyaura coupling (SMC) reaction

All experiments to evaluate the catalytic activity were performed under air in a round bottomed flask, unless mentioned. In a general reaction procedure, the catalyst was weighed into the flask followed by the addition of a base, phenylboronic acid and the substrate (bromobenzene or chlorobenzene) in a molar ratio of 4 : 3 : 2. The solvent (5 mL) was added to disperse the

reactants well and the flask was mounted on a preheated oil bath at T K and the reaction was continued for t h. After the passage of desired time, the flask was allowed to cool to room temperature and naphthalene was added as an internal standard. The reaction mixture was stirred at room temperature, diluted and the catalyst was filtered off using a Milex®-LG 0.20 μm . The obtained filtrate was analyzed by gas chromatography (GC-17A, Shimadzu Co.) using an Agilent DB-1 column (30 m \times 0.25 mm \times 0.25 μm) attached to a FID detector. The conversion and selectivity were determined with a calibration curve method using naphthalene as an internal standard.

Recycling tests were performed to check the stability of the Pd/AZC catalysts during the reaction. The catalyst was separated from the reaction mixture by centrifugation. The supernatant liquid was stored, and then analysis of products and the leaching test of catalysts were performed. The residual catalyst and base were washed by centrifugation with ethanol and dried *in vacuo* overnight. Fresh substrates and reagents were added to the catalyst, and then the reusability of the catalyst was verified under similar reaction conditions.

In a typical case of isolation of 4-phenylbenzoic acid (Table 2, entry 4), naphthalene was not added to the reaction mixture. The reaction mixture was centrifuged and the resulting supernatant liquid was filtered to remove any suspended solid particles. The ethanol solution was concentrated followed by the addition of water to precipitate the organics. The reaction mixture containing water, ethanol and white solid were centrifuged again and the supernatant liquid was collected separately to remove traces of bromobenzene (liquid). The solid was dissolved in a very small amount of ethanol and sufficient water was added to achieve precipitation and was then centrifuged. The mixture was left overnight to obtain colourless crystals to record ^1H NMR spectra.

Table 1 The SMC reaction with the Pd/AZC catalyst^a

Entry	X	R	Catalyst	Pd ^b /μmol	Time/h	Yield ^c /%
1	Br	H	0.5 Pd/AZC	1.4	0.5	>99
2				23.5×10^{-2}		93
3 ^d			0.05 Pd/AZC	4.7×10^{-3}	48	>99
4			0.5 Pd/AZC	4.7×10^{-2}	1.0	77, 75, ^e 85 ^f
5 ^g				1.4		0
6 ^h	Cl	NO ₂	3 Pd/AZC	1.4	3.0	>99
7 ^{h,i}	Cl	H		5.6	4.0	18
8 ^{h,i,j}				2.8	6.0	34

^a Reaction conditions: substrate (2 mmol), phenylboronic acid (3 mmol), K₂CO₃ (4 mmol), ethanol (5 mL), round bottomed flask, 353 K, air. ^b Actual amount of Pd used in the reaction estimated by ICP-AES. ^c Determined by GC using naphthalene as the internal standard on the basis of bromobenzene. ^d Bromobenzene (10 mmol). ^e 1st reuse. ^f 2nd reuse. ^g Without bromobenzene. ^h Substrate (0.5 mmol), phenylboronic acid (0.75 mmol), K₂CO₃ (1 mmol), ethanol, 353 K. ⁱ In the presence of tetrabutylammonium bromide (TBAB; 1 mmol). ^j Ethanol : DMF (1 : 1), 50 mL Teflon lined autoclave, 373 K.

2.5 Heterogeneity test and solid-phase poisoning test

2.5.1 Hot filtration test. 0.5 wt% Pd/AZC (1 mg) was weighed into the flask followed by K₂CO₃ (4 mmol), phenylboronic acid (3 mmol) and bromobenzene (2 mmol). Finally ethanol (5 mL) was added to disperse the reactants and the reaction mixture was heated at 353 K. After 20 minutes of reaction progress, naphthalene (as an internal standard) was added and the catalyst was separated at the reaction temperature by centrifugation followed by filtration using a Milex®-LG 0.20 μm . An additional amount of K₂CO₃ (3 mmol) was introduced to the filtrate and the reaction was continued at 353 K for an additional 40 minutes.

Furthermore, as a separate experiment 0.5 wt% Pd/AZC (1 mg) was weighed in to the flask followed by the addition of the base, phenylboronic acid and bromobenzene in a molar ratio of 4 : 3 : 2 and ethanol (5 mL). The resulting solution was stirred at 353 K for 1 h. After 1 h of reaction progress, naphthalene was added and subjected to GC analysis. The catalyst was removed by centrifugation followed by filtration using a Milex®-LG 0.20 μm and fresh reagents (base, phenylboronic acid and bromobenzene in a molar ratio of 4 : 3 : 2) were added and the reaction was continued for another 1 h at 353 K. The product concentration was determined by GC analysis.

2.5.2 Solid-phase poisoning test. The catalyst poison candidate was added to the reaction flask before the addition of the reagents for the SMC reaction of bromobenzene. The amount of QuadraPure® TU was used four times of that required to bind total Pd as indicated by the manufacturer (scavenging limit; 0.19 mmol Pd per gram QuadraPure TU). As a control experiment aq. PdCl₂ (47 nmol Pd) was used as the catalyst with two equivalents of QuadraPure TU (twice the amount required to bind all the palladium in the reaction mixture).

2.6 Characterization

The structure was analyzed by powder X-ray diffraction (PXRD) patterns with a SmartLab (Rigaku Co.) using Cu K α radiation (λ = 0.154 nm) at 40 kV and 30 mA in the range of 2θ = 4–60°. The diffraction patterns were analyzed with the database in the joint committee of powder diffraction standards (JCPDS). For inductively coupled plasma atomic emission spectroscopy (ICP-AES) analysis, an ICPS-7000 ver. 2 (Shimadzu Co.) was employed to quantify the actual Pd amount and to evaluate Pd leaching, if any, during the reaction. Contents of Pd in the catalyst and/or the reaction medium were estimated by a calibration curve method. A H-7100 (Hitachi, Ltd.) operating at 100 kV was utilized to acquire the morphology of the catalyst by transmission electron microscopy (TEM). The samples for TEM measurements were dispersed in water or ethanol, and the supernatant liquid was dropped onto a copper grid before drying *in vacuo* overnight. Scanning electron microscopy (SEM) micrographs were obtained using an S-4100 (Hitachi, Ltd.). The electronic state of Pd and Zn was analyzed by X-ray photoelectron spectroscopy (XPS). The XPS experiments were conducted on an AXIS-ULTRA DLD spectrometer system (Shimadzu Co. and Kratos Analytical Ltd.) using an Al target at 15 kV and 10 mA.

Table 2 The SMC reaction of aryl halides and boronic acids with the Pd/AZC catalyst^a

Entry	X	R ₁	R ₂	R ₃	Time/h	Conv. ^b /%	Yield ^b /%
1	Br	H	H	H	1.0	80	77
2				OCH ₃		83	69
3				F		91	92
4 ^c				COOH	3.0	84	73 ^{f,g}
5 ^d	Cl	NO ₂	H	H		>99	>99
6 ^d				OCH ₃		26	19 ^g
7 ^d				F		47	32 ^{g,h}
8	I	H	H	H	0.3	99	96
9				OCH ₃	1.0	>99	68
10				F		90	89
11 ^e		COOH	OH	H	3.0	82	76 ^g

^a Reaction conditions: aryl halide (2 mmol), boronic acid (3 mmol), K₂CO₃ (4 mmol), 0.5 Pd/AZC (1 mg), ethanol (5 mL), round bottomed flask, 353 K, air. ^b Determined by GC using naphthalene as the internal standard on the basis of aryl halides. ^c Aryl halide (1 mmol), boronic acid (1.5 mmol), K₂CO₃ (2 mmol), 0.5 Pd/AZC (5 mg). ^d Aryl halide (0.5 mmol), boronic acid (0.75 mmol), K₂CO₃ (1 mmol), 3 Pd/AZC (5 mg). ^e 0.5 Pd/AZC (5 mg). ^f Isolated yield. ^g Product was confirmed by NMR and GC-MS (see the ESI). ^h 4,4'-Difluorobiphenyl was observed.

in an energy range of 0–1200 eV. The binding energies were calibrated with the O 1s level (531.0 eV) as an internal standard reference. X-ray absorption spectroscopy (XAS) was performed with a transmission and/or fluorescence mode at a BL-9C in KEK-PF under the approval of the Photon Factory Program Advisory Committee (Proposal no. 2013G586) and BL01B1 in SPring-8 under the approval of the Japan Synchrotron Radiation Research Institute (JASRI) (Proposal no. 2012B1610 and 2013B1478). The obtained XAS spectra were analyzed with Rigaku REX2000 software (ver. 2.5.92). The IR measurements of samples were carried out on a PerkinElmer Spectrum 100 FT-IR spectrometer. Nuclear Magnetic Resonance (NMR) spectra were recorded on a 400 MHz Bruker (AVANCE III 400) using DMSO-d₆ as the solvent with TMS as the internal standard. A gas Chromatogram (GC-17A, Shimadzu Co.) coupled to a Mass Spectrometer (QP5000, Shimadzu Co.) (GC-MS) was employed to obtain the mass fragmentation spectra of synthesized compounds.

3. Results and discussion

3.1 Morphology and crystallinity of AZC and Pd/AZC

Solvothermal treatment of Zn(NO₃)₂·6H₂O with ATA in DMF at 413 K, followed by ethanol treatment afforded a brownish material (denoted as AZC). The SEM (Fig. 1a) and TEM (Fig. 1b) analyses of the sample captured porous blocks with an irregular size and shape having thread/tube like features at the edges. The AZC and Pd/AZC consisted of a phase with PXRD patterns observed at 2θ = 11.2, 14.4, 18.1, 20.3, 23.6, 25.8 and 27.2° corresponding to (111), (210), (220), (310), (320), (400) and (411) planes, respectively (Fig. 2), which were much different from the

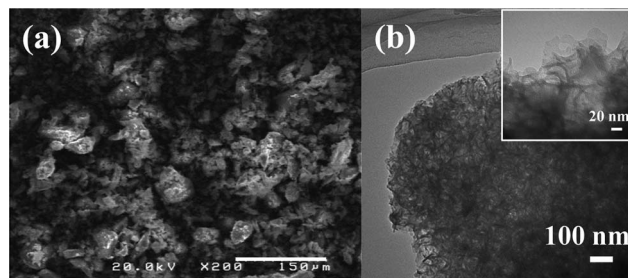


Fig. 1 (a) SEM micrograph of AZC showing irregular blocks. (b) TEM images of AZC at different magnifications.

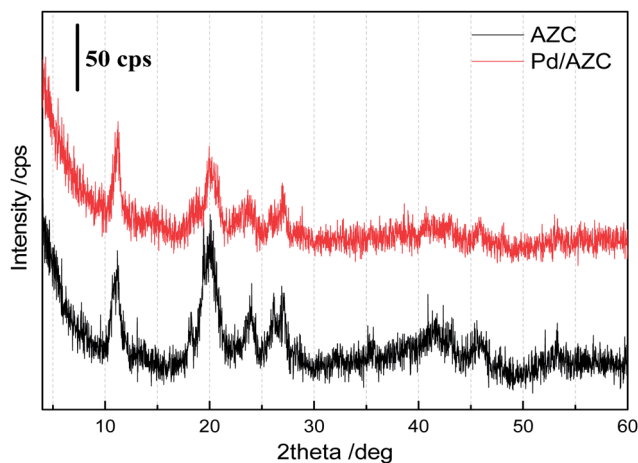


Fig. 2 XRD patterns of AZC (black) and Pd/AZC (red).

PXRD patterns of IRMOF-3 and MIL-53 reported, previously.^{2,46} Requisite amounts of PdCl_2 were loaded on AZC by an adsorption method to afford $x\text{Pd}/\text{AZC}$, where the x is the Pd content (wt%) in theory. The Pd grafting process on AZC preserved its original structure as evidenced by XRD (Fig. 2). The co-existence of agglomerates and large crystals of impurities such as ZnO , PdCl_2 and PdO in these materials were excluded on the basis of TEM images and XRD patterns.

3.2 Catalytic activity of Pd/AZC for the SMC reaction

The catalytic activity of Pd/AZC was investigated for the SMC reaction and was found to be highly active for both bromo- and chloro-benzenes (Table 1). All experiments were performed under an air atmosphere. High activities for bromobenzene were realized at a shorter reaction time even with low Pd loading (Table 1, entries 1–2). Although some of the current reports have demonstrated a highly efficient SMC reaction in aqueous media, we found our catalytic system to be fruitful in the ethanol solvent (see ESI, Table S1†). While optimizing the activity of Pd/AZC in ethanol, a remarkable TON value of 2 106 720 was reached with 4.7 nmol of Pd for 10 mmol of bromobenzene (Table 1, entry 3, and also see Table S2 in the ESI†). The highly active Pd/AZC could keep its potential at least up to recycling 7 runs without any significant loss of activity (Table 1, entry 4, and Fig. S1 in ESI†). The control experiment without bromobenzene (Table 1, entry 5) pronounced the catalytic activity to be restricted to cross-coupling under the present reaction conditions.

The activity was not limited to bromobenzene; the reaction of activated chlorobenzene (*p*-nitrochlorobenzene) also afforded 4-nitrobiphenyl with >99% yield (>99% conv.) in the absence of additives (Table 1, entry 6). However, we realized that chlorobenzene could not be coupled effectively with arylboronic acid under the present reaction conditions (Table S3 in the ESI†), whereas a higher conversion of chlorobenzenes (58.4%) was observed at 353 K in the presence of TBAB with 18% yield of biphenyl (Table 1, entry 7). In fact, chloroarenes required larger Pd amounts in comparison to bromoarenes. Employment of ethanol and DMF as solvents with TBAB as the additive agent^{47,48} could improve the yield of biphenyl moderately in an autoclave reactor (Table 1, entry 8); the implementation of such reaction parameters in an autoclave could afford high conversion of chlorobenzene with decent yields (30–34%) of biphenyl (see the ESI, Table S3†).

For future interests, not only the various aryl halides but also their reactivity with diverse boronic acids was subjected to the SMC reaction using the Pd/AZC catalyst. These reactions were also attempted and are tabulated in Table 2.

The reactivities of aryl halides in general were found to decrease with the use of phenylboronic acids (Table 2, entries 1, 5, 8; $\text{R}_3 = \text{H}$) to fluorophenylboronic acids (entries 3, 7, 10; $\text{R}_3 = \text{F}$) to methoxyphenylboronic acids (Table 2, entries 2, 6, 9; $\text{R}_3 = \text{OCH}_3$). Because of the high reactivity of fluorophenylboronic acid, a large excess of the palladium catalyst and low reactivity of aryl chloride produced 4,4'-difluorobiphenyl as the homocoupling product of fluorophenylboronic acid in traces

(Table 2, entry 7). The cross-coupling of 4-carboxyphenylboronic acid with bromobenzene required longer reaction times and higher amounts of palladium to accomplish decent yields (Table 2, entry 4). The 2 mmol iodobenzene quickly cross-coupled with phenylboronic acid to produce >90% biphenyl yields within 20 minutes catalyzed by 47 nmol of palladium, whereas in contrast, aryl iodides with hydroxyl and carboxyl functional groups necessitated longer reaction times to reach high conversions (Table 2, entries 8, 11).

3.3 Investigation of the localized Pd/AZC structure around the Zn atom

To account for the high activity and propose a suitable mechanistic pathway for the SMC reaction over Pd/AZC, the structural features were further characterized by spectroscopic methods. The local structure around zinc in AZC and palladium in Pd/AZC was investigated by XAS measurements. The Zn *K*-edge X-ray absorption near-edge structure (XANES) spectrum of AZC was similar to the Zn(II) salts of $\text{Zn}(\text{OAc})_2$ and $\text{Zn}(\text{NO}_3)_2 \cdot 6\text{H}_2\text{O}$ (Fig. 3a); 58% of $\text{Zn}(\text{OAc})_2$ with 42% of $\text{Zn}(\text{NO}_3)_2 \cdot 6\text{H}_2\text{O}$ was estimated by deconvolution of XANES features (see the ESI, Fig. S2†), indicating the Zn(II) species as the integral part of electronic states and/or the local structure in AZC.

XPS analysis of AZC also indicated that the Zn has an oxidation state of +2 observed at 1021.4 eV (see the ESI, Fig. S3†).⁴⁹ The k^3 -weighted extended X-ray absorption fine structure (EXAFS) of AZC at the Zn *K*-edge suggested a high similarity in EXAFS oscillation to $\text{Zn}(\text{OAc})_2$; merging estimation

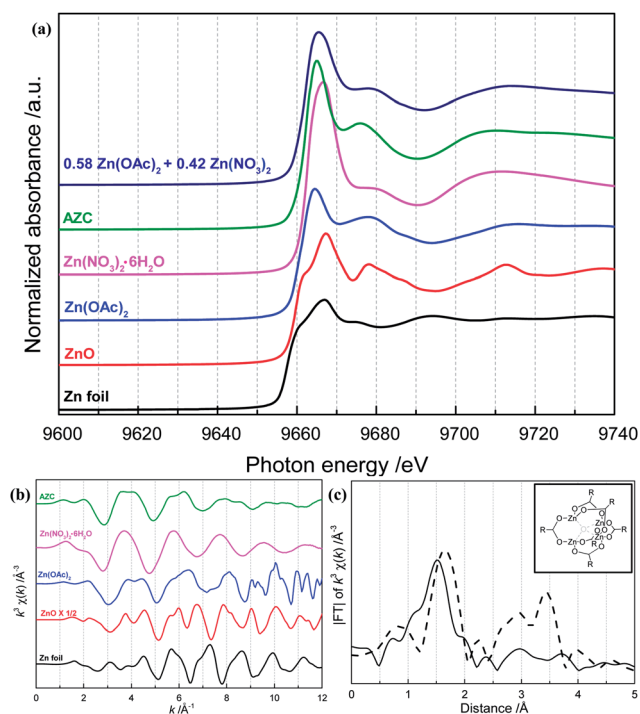


Fig. 3 (a) Normalized XANES (b) EXAFS spectra at the Zn *K*-edge of references and AZC. (c) FT of the k^3 -weighted EXAFS spectrum of AZC (solid line) and $\text{Zn}(\text{OAc})_2$ (dashed line) at the Zn *K*-edge. The inset shows the proposed local structure around Zn in AZC.

indicated that the AZC has structural features of $\text{Zn}(\text{OAc})_2$ (above 80%) mixed with $\text{Zn}(\text{NO}_3)_2 \cdot 6\text{H}_2\text{O}$ (Fig. 3b, and see the ESI, Fig. S4†). A broad peak in the Fourier transforms (FT) of EXAFS of AZC appeared at 1.3–1.7 Å (solid line, Fig. 3c) and which was at lower distance of Zn–O coordination compared to $\text{Zn}(\text{OAc})_2$ (dashed line, Fig. 3c). This shift towards lower bond distance in AZC was supposedly accounted due to differences in the side-chain of RCOO^- ($\text{R} = \text{CH}_3$ in $\text{Zn}(\text{OAc})_2$ and $\text{C}_6\text{H}_3(\text{NH}_2)(\text{COOH})$ in AZC) and structural complexity relating to higher bond strength of Zn–O.

3.4 Investigation of the localized Pd/AZC structure around the Pd atom

The IR analysis of AZC and Pd/AZC demonstrated that ATA was stable under synthesis conditions forming a palladium–amine complex assembly (N–H and Pd–N stretching was observed) (Fig. 4a and S5 in the ESI†). The appearance of two peaks (at 477 and 496 cm^{-1}) for Pd–N in IR spectra supports the loading of Pd on AZC through the palladium–amine complex with *cis* geometry.⁵⁰ In the Pd 3d XPS shown in Fig. 4b, the peaks at higher binding energy (than that of Pd foil) distinguished the oxidized/ionic species of palladium in Pd/AZC. Deconvolution analysis of

the XPS of Pd/AZC in the Pd 3d region: Pd $3d_{3/2}$ (342.2 eV) and $3d_{5/2}$ (336.9 eV), split each individual peak into two peaks at 341.4 eV and 342.3 eV for Pd $3d_{3/2}$ whereas 335.6 eV and 337.1 eV for Pd $3d_{5/2}$; corresponding to Pd(II) in the square planar organopalladium complex and oxygen-coordinated Pd(II) states (Fig. 4b).^{51,52} The Pd *K*-edge XAS studies of the Pd/AZC were also performed, and its oxidation states as well as co-ordination of Pd species were estimated. Pd *K*-edge XANES characteristics

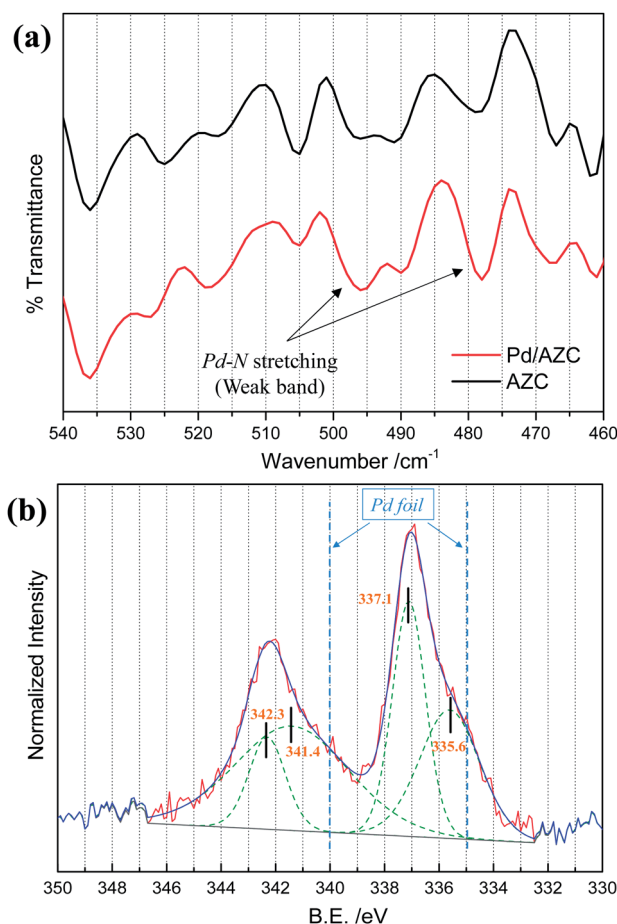


Fig. 4 (a) IR spectrum of AZC (black) and Pd/AZC (red) demonstrating the two weak Pd–N stretching observed for Pd/AZC. (b) XPS of Pd 3d in Pd/AZC.

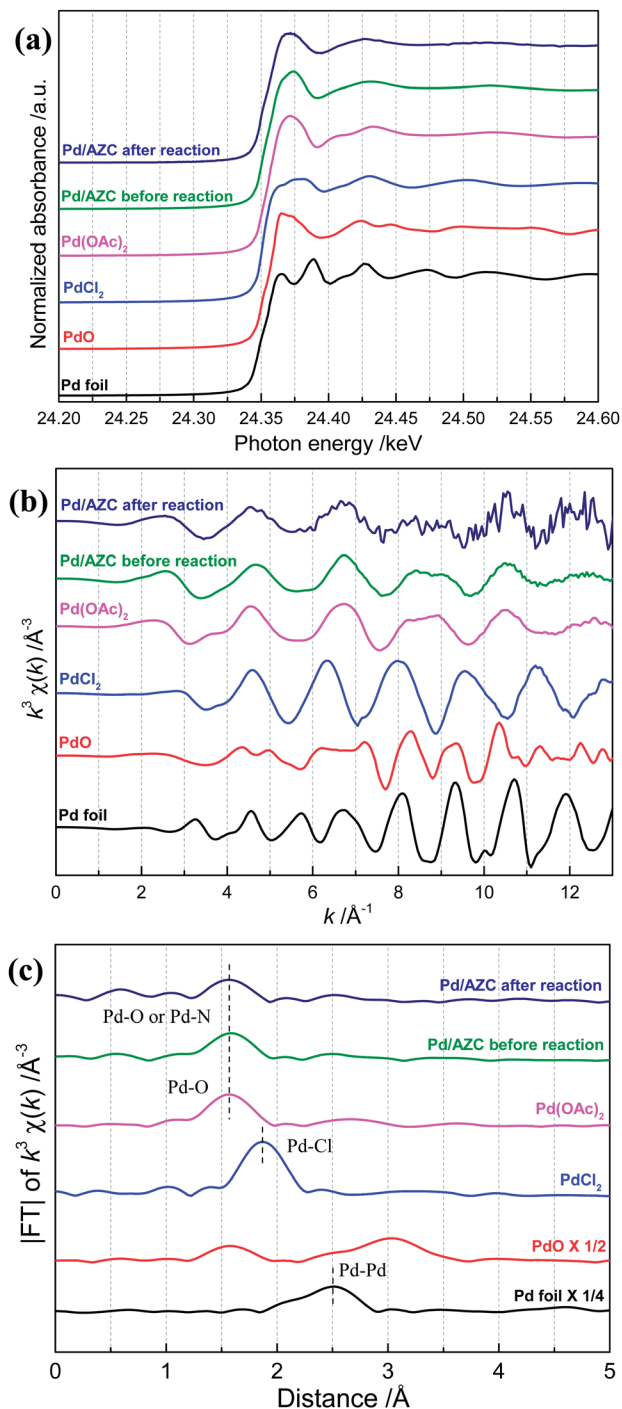


Fig. 5 (a) Normalized XANES, (b) k^3 -weighted EXAFS and (c) FT of k^3 -weighted EXAFS of references and Pd/AZC at Pd *K*-edge XAS.

(Fig. 5a), EXAFS (Fig. 5b), and FT of EXAFS (Fig. 5c) of Pd/AZC were very different from the Pd foil but had resemblance to the Pd(II) state of Pd(OAc)₂ (Fig. 6a). The literature survey suggested the species to possess a square planar geometry close to that of Pd(OAc)₂ or [Pd(NH₃)₄]Cl₂.⁵³ The FT of EXAFS exhibited a single peak in the region of 1.4–1.8 Å (Fig. 6a), resulting from the backscattering of the adjacent nitrogen and/or oxygen atoms (Fig. 5b and c). The inverse FT of the peak was well-fitted using Pd–N (CN = 1.8) and Pd–O (CN = 2.2) shells in the range of $k = 4$ –12 Å^{−1} (Fig. 6b and Table 3). Mori *et al.*⁵⁴ reported the loading

of Pd on hydroxyapatite (HAP) with Pd coordinated to four oxygens in a Ca-deficient site of HAP. A sound similarity in the FT of Pd/AZC and PdHAP⁵⁴ at Pd *K*-edge were observed.

3.5 Proposed structure of Pd/AZC

The local structure around the Pd atom was proposed as shown in Fig. 7. Neither any characteristics peak for the Pd–Pd bond, nor any significant signals at higher distances were observed in FT, supporting the monomeric atomically dispersed Pd ions with AZC. A thoughtful conclusion of these characteristics data inspired us to propose the structures of AZC and Pd/AZC as described in Fig. 7. A detailed and minute study with higher accuracy for structural determination is subject to further investigation and ongoing work.

3.6 Heterogeneity of the Pd/AZC catalyst during the SMC reaction

The Pd *K*-edge XANES and EXAFS analysis of the catalyst after the SMC reaction (of bromo- and chlorobenzene) suggested that the catalyst conserved its original structural features (Fig. 5a–c). EXAFS oscillation of the spent catalyst was indistinguishable from the fresh catalyst. Besides, the FT of k^3 -weighted EXAFS at the Pd *K*-edge denied the presence of any Pd–Pd shell in the spent catalyst, rather bespoke the ionic Pd species with signals for Pd–N/Pd–O shells. XRD patterns of the catalyst after the reaction also supported the integrity of the catalyst after the reaction (see the ESI, Fig. S6†). The ICP-AES analysis confirmed that neither the supported Pd nor the assembled Zn leached during the SMC reaction under our reaction conditions on the ppm order.

The hot-filtration test is a useful method for establishing the heterogeneity of the catalytic reaction. After 20 minutes of SMC reaction progress, the catalyst was quickly filtered off (see Section 2.5) and the filtrate along with an additional base was stirred for another 40 minutes at 353 K. The GC analysis showed a high initial rate of reaction with 60% biphenyl yield (62% conv.) within 20 minutes of the reaction with just 1 mg of 0.5 wt% Pd/AZC. The SMC reaction did not proceed after the separation of the solid catalyst after 20 minutes. Additionally, in a separate experiment when fresh reactants (bromobenzene, phenylboronic acid and base with the molar ratio of 2 : 3 : 4) were added to the filtrate obtained by centrifugation and filtration with the filter (0.2 μm) after 1 h of the SMC reaction, further reaction did not take place. These results indicate that the catalysis by Pd/AZC is heterogeneous.

As described by various researchers,^{55–59} the solid-phase poisoning tests were performed to ascertain the heterogeneity of Pd/AZC in the SMC reaction. Richardson and Jones reported that two equivalents of QuadraPure TU which are required for binding all the palladium could completely shutdown the reactivity of solid catalysts that operate through the leaching mechanism.⁵⁶ In our case, however, it was found that the use of even four equivalents of QuadraPure TU could not affect the catalytic activity of Pd/AZC. The control experiment with aq. PdCl₂ and two equivalents of QuadraPure TU afforded no product with 4% bromobenzene conversion. It confirms that no

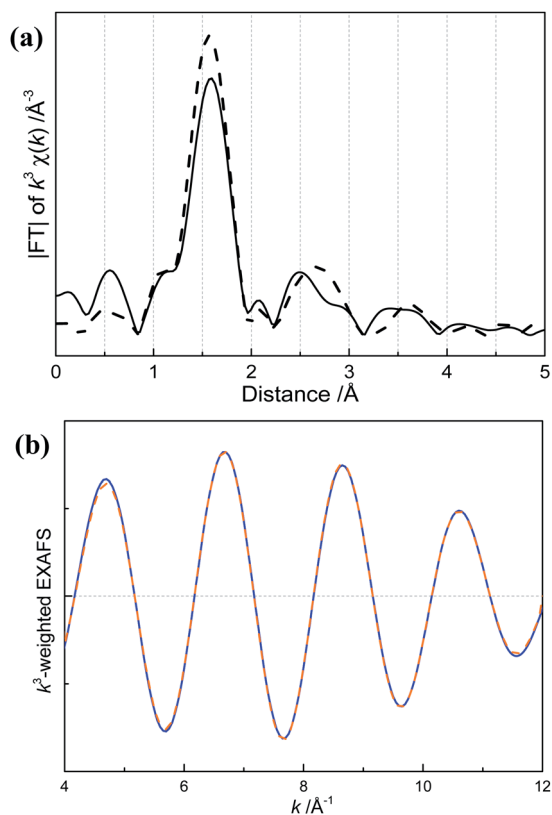


Fig. 6 (a) FT of the k^3 -weighted EXAFS spectrum of Pd/AZC (solid line) and Pd(OAc)₂ (dashed line) at the Pd *K*-edge. (b) The inverse FT of Pd/AZC performed in the range of 4–12 Å^{−1}. The dashed orange line shows the results of a curve-fitting analysis.

Table 3 Curve-fitting results for Pd *K*-edge EXAFS^a

Shell	CN ^b	R ^c /Å	DW ^d /Å ²
Pd–N	1.8	2.050	0.0004
Pd–O	2.2	2.026	0.0104

^a The curve fitting was performed using the McKale method. FT of the k^3 -weighted EXAFS spectrum ($k^3\chi(k)$) of Pd/AZC was performed in the range of $k = 3$ –13 Å^{−1} with a window function for 20, and the inverse FT was examined in the ranges of $k = 4$ –12 Å^{−1} and $R = 1.258$ –1.872 Å with a window function for 10. The obtained results were under the *R* factor of 0.041%; which was defined by the formula $\frac{\sum (k^3\chi_{\text{obs}} - k^3\chi_{\text{cal}})^2}{\sum (k^3\chi_{\text{obs}})^2}$. ^b Coordination number. ^c Interatomic distance.

^d Debye–Waller factor.

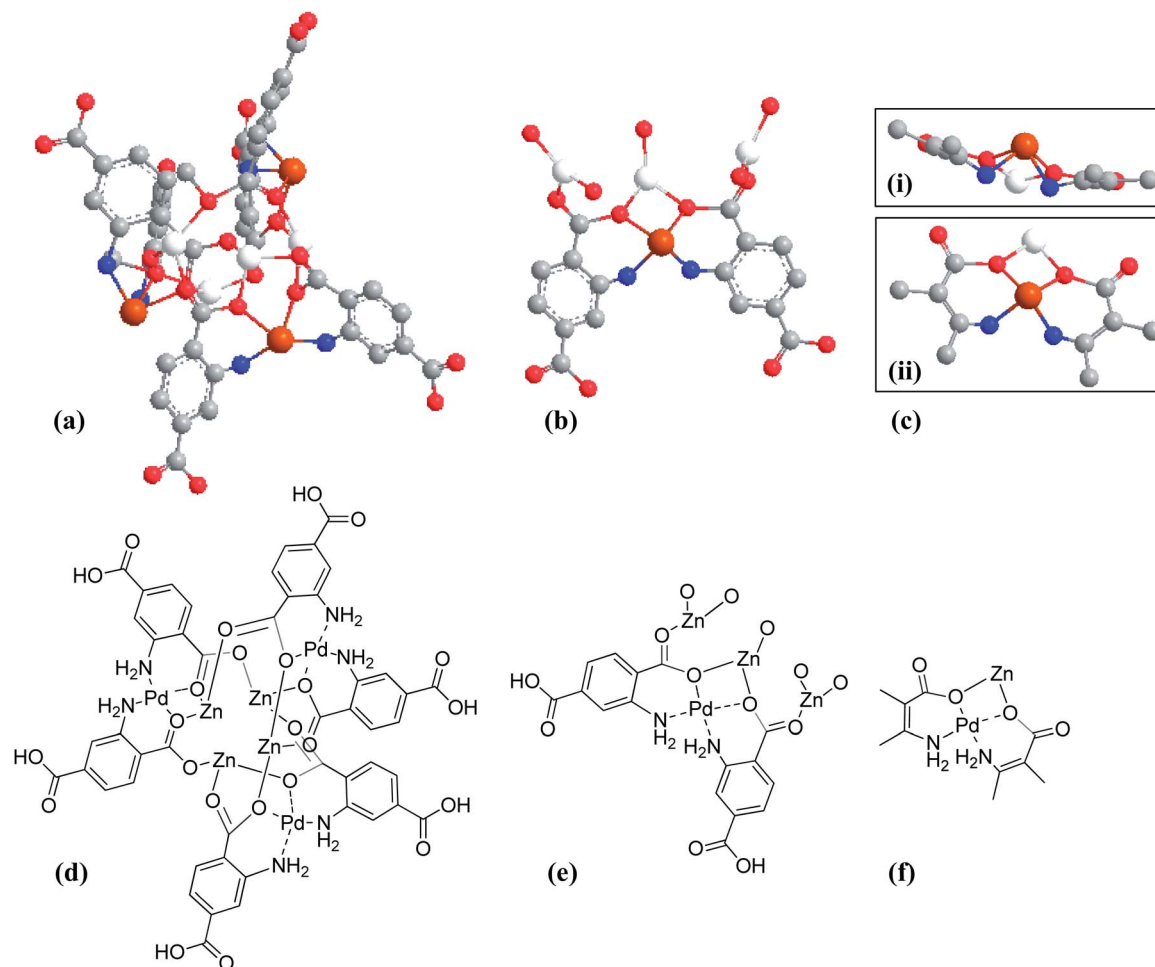


Fig. 7 Proposed structure of AZC on the basis of spectroscopic characterization. Ball and stick model structure of (a) Pd/AZC; (b) local structure around palladium and zinc in Pd/AZC; (c) (i) side and (ii) top view of the local structure of palladium in Pd/AZC. (d)–(f) Simplified structure of (a)–(c). Carbon (gray), oxygen (red), nitrogen (blue), palladium (brown), and zinc (white). The hydrogen atoms are not shown for simplicity in the ball and stick model.

homogeneous Pd species catalyze the SMC reaction under our conditions. These experiments authenticated the significant heterogeneous nature of the Pd/AZC catalyst.

Even after two decades of the SMC reaction, it is still a matter of discussion that whether the genuine catalysis by the heterogeneous catalyst is heterogeneous or homogeneous. Some researchers have held the atom-leaching mechanism as the main cause of high activity for such cross-coupling reactions.^{55,60,61} The non-leaching of the palladium species into the reaction medium is supposed to be the reason for low activity (34% biphenyl yield) of chlorobenzene in the present case. As discussed above, no black-colored Pd or reduced Pd was observed after the SMC reaction over Pd/AZC and this reflects the stability of heterogeneous Pd/AZC. The results also indicate that the Pd precipitation during the reaction and its effect on catalytic activity of Pd species could be negligible with enduring AZC as the support. The strong affinity of Pd to N and interaction of ionic Pd with oxygen could prevent the active Pd species from leaching or undergo agglomeration under the reaction conditions.

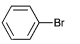
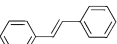
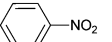
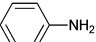
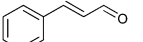
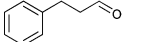
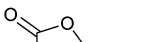
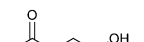
3.7 Proposed reaction pathway

A general reaction mechanism by divalent Pd has been considered and sketched accordingly (see the ESI, Scheme S1†). An oxidative addition of bromobenzene on the exposed Pd(II) center of $\text{Pd}(\text{O})_2(\text{NH}_3)_2$ followed by ligand exchange with the base and arylboronic acid are considered as sequential steps. Reductive elimination of biphenyl regenerates the active naked Pd and thereby the hetero-coupling of bromoarenes and arylboronic acid takes place consecutively. Since the active Pd species is generated, no further regeneration step is required and thus the product with a high TON is afforded.

3.8 Catalytic scope of Pd/AZC for other organic reactions

The Pd/AZC catalyst was also used for various Pd-catalyzed reactions as shown in Table 4. We found that the present Pd/AZC catalyst efficiently catalyzed the Mizoroki–Heck reaction of bromobenzene and styrene (Table 4, entry 1). The catalyst also efficaciously promoted hydrogenation reactions of the $-\text{NO}_2$ group (in nitrobenzene), and the $-\text{C}=\text{C}-$ group (in

Table 4 Scope of catalysis by Pd/AZC

Entry	Substrate	Product	Time/h	Conv. ^a /%	Yield ^a /%
1 ^b	 bromobenzene	 <i>trans</i> -stilbene	24	97	84
2 ^c	 nitrobenzene	 aniline	2.5	>99	>99
3 ^c	 cinnamaldehyde	 3-phenylpropanol	6	>99	>99
4 ^{c,d,e}	 maleic anhydride	 succinic acid	6	>99	98

^a Determined by GC using naphthalene as the internal standard.

^b Reaction conditions: bromobenzene (3.75 mmol), styrene (4.5 mmol), K₂CO₃ (4.5 mmol), 0.5 Pd/AZC (25 mg), 1-methyl-2-pyrrolidinone (5 mL), 403 K, N₂ flow. ^c Reaction conditions: substrate (1 mmol), 3 Pd/AZC (25 mg), ethanol (5 mL), H₂ balloon (1 atm), 353 K. ^d Water was used instead of ethanol. ^e The conversion and yield were determined using HPLC (Waters 600).

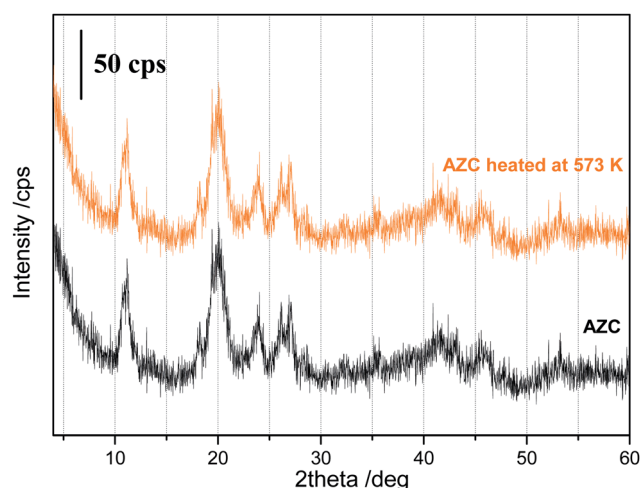


Fig. 8 XRD patterns of AZC (black) and AZC heated at 573 K (orange).

cinnamaldehyde and maleic anhydride) under mild conditions using hydrogen at an atmospheric pressure (Table 4, entries 2–4). Since the structure of AZC is stable against heat treatment (at least up to 573 K) (Fig. 8), the synthesized support (AZC) is believed to be capable of grafting various metal species as catalytically active centers for a wide range of industrially important metal-catalyzed reactions.

4. Conclusions

In conclusion, we found that ionic palladium species grafted on an amino-functionalized organozinc coordination polymer (Pd/AZC) served as a robust catalyst for the SMC reaction for bromobenzene. The reusable Pd/AZC demonstrated impressive

high turnover numbers (TON = 2 106 720) without any additives under atmospheric conditions. The SMC reaction of other aryl halides and aryl boronic acids could also be efficaciously catalyzed by Pd/AZC under similar conditions. The characterization evidences the stability and durability of the Pd/AZC catalyst, highlighting it as a candidate for a potential industrial catalyst.

The Pd/AZC also successfully catalyzed the Mizoroki–Heck coupling, hydrogenation of nitro, and –C=C– functional groups. The high thermal stability, reflect its high potential for grafting various metal species as catalytically active centers for a wide range of metal-catalyzed reactions.

Acknowledgements

The authors are thankful to Prof. Dr Yuki Nagao (JAIST) for helpful discussion on the AZC morphology and Prof. Dr Tetsuya Shishido (Tokyo Metropolitan Univ.) for support in XAS measurements. HC extends his thanks to the Japan Society for the Promotion of Science (JSPS) for the fellowship. This work is partially supported by JSPS KAKENHI Grant Numbers 26-12396 (Grant-in-Aid for JSPS Fellows) and 25820392 (Grant-in-Aid for Young Scientists (B)).

Notes and references

- O. M. Yaghi, H. Li and T. L. Groy, *J. Am. Chem. Soc.*, 1996, **118**, 9096.
- M. Eddaoudi, J. Kim, N. Rosi, D. Vodak, J. Watcher, M. O’Keeffe and O. M. Yaghi, *Science*, 2002, **295**, 469.
- S. Kitagawa, R. Kitamura and S. Noro, *Angew. Chem., Int. Ed.*, 2004, **43**, 2334.
- N. Miyaoura, K. Yamada and A. Suzuki, *Tetrahedron Lett.*, 1979, **20**, 3437.
- N. Miyaoura, T. Yanagi and A. Suzuki, *Synth. Commun.*, 1981, **11**, 513.
- N. Miyaoura and A. Suzuki, *Chem. Rev.*, 1995, **95**, 2457.
- A. Suzuki, *J. Organomet. Chem.*, 2002, **653**, 83.
- A. F. Littke and G. C. Fu, *Angew. Chem., Int. Ed.*, 2002, **41**, 4176.
- A. Molnar, *Chem. Rev.*, 2011, **111**, 2251.
- C.-J. Li, *Chem. Rev.*, 2005, **105**, 3095.
- S. Grunder, C. Valente, A. C. Whalley, A. Sampath, J. Portmann, Y. Y. Botros and J. F. Stoddart, *Chem.-Eur. J.*, 2012, **18**, 15632.
- K.-Y. Park, B. T. Kim and J.-N. Heo, *Eur. J. Org. Chem.*, 2014, 164.
- K. D. Hesp, D. P. Fernando, W. Jiao and A. T. Londregan, *Org. Lett.*, 2014, **16**, 413.
- V. Polshettiwar and R. S. Varma, *Chem. Soc. Rev.*, 2008, **37**, 1546.
- V. Polshettiwar and R. S. Varma, *Acc. Chem. Res.*, 2008, **41**, 629.
- C. Deraedt and D. Astruc, *Acc. Chem. Res.*, 2014, **47**, 494.
- M. Pittelkow, K. Moth-Poulsen, U. Boas and J. B. Christensen, *Langmuir*, 2003, **19**, 7682.
- J.-H. Li and W.-J. Liu, *Org. Lett.*, 2004, **6**, 2809.

- 19 Z. Weng, S. Teo and T. S. A. Hor, *Acc. Chem. Res.*, 2007, **40**, 676.
- 20 A. K. Diallo, C. Ornelas, L. Salmon, J. R. Aranzaes and D. Astruc, *Angew. Chem., Int. Ed.*, 2007, **46**, 8644.
- 21 F. X. L. Xamena, A. Abad, A. Corma and H. Garcia, *J. Catal.*, 2007, **250**, 294.
- 22 S. Jana, S. Halder and S. Koner, *Tetrahedron Lett.*, 2009, **50**, 4820.
- 23 K. Okumura, T. Tomiyama, S. Okuda, H. Yoshida and M. Niwa, *J. Catal.*, 2010, **273**, 156.
- 24 S. Ogasawara and S. Kato, *J. Am. Chem. Soc.*, 2010, **132**, 4608.
- 25 J. Zhi, D. Song, Z. Li, X. Lei and A. Hu, *Chem. Commun.*, 2011, **47**, 10707.
- 26 Y. Yu, T. Hu, X. Chen, K. Xu, J. Zhang and J. Huang, *Chem. Commun.*, 2011, **47**, 3592.
- 27 P. M. Uberman, L. A. Perez, G. I. Laconi and S. E. Martin, *J. Mol. Catal. A: Chem.*, 2012, **363–364**, 245.
- 28 Y. M. A. Yamada, S. M. Sarkar and Y. Uozumi, *J. Am. Chem. Soc.*, 2012, **134**, 3190.
- 29 D. Saha, R. Sen, T. Maity and S. Koner, *Langmuir*, 2013, **29**, 3140.
- 30 C. Deraedt, L. Salmon, L. Etienne, J. Ruiz and D. Astruc, *Chem. Commun.*, 2013, **49**, 8169.
- 31 X. Pan, Z. Fan, Z. Chen, Y. Ding, H. Luo and X. Bao, *Nat. Mater.*, 2007, **6**, 507.
- 32 X. Chen, Y. Hou, H. Wang, Y. Cao and J. He, *J. Phys. Chem. C*, 2008, **112**, 8172.
- 33 E. Castillejos, P.-J. Deboutiere, L. Roiban, A. Solhy, V. Martinez, Y. Kihn, O. Ersen, K. Philippot, B. Chadret and P. Serp, *Angew. Chem., Int. Ed.*, 2009, **48**, 2529.
- 34 B. Cornelio, G. A. Rance, M. Laronze-Cochard, A. Fontana, J. Sapi and A. N. Khlobystov, *J. Mater. Chem. A*, 2013, **1**, 8737.
- 35 B. Yuan, Y. Pan, Y. Li, B. Yin and H. Jiang, *Angew. Chem., Int. Ed.*, 2010, **49**, 4054.
- 36 J. Huang, W. Wang and H. Li, *ACS Catal.*, 2013, **3**, 1526.
- 37 A. Corma, H. Garcia and A. Leyva, *Appl. Catal., A*, 2002, **236**, 179.
- 38 S. Mandal, D. Roy, R. V. Chaudhari and M. Sastry, *Chem. Mater.*, 2004, **16**, 3714.
- 39 M.-J. Jin, A. Taher, H.-J. Kang, M. Choi and R. Ryoo, *Green Chem.*, 2009, **11**, 309.
- 40 R. Zhang, W. Ding, B. Tu and D. Zhao, *Chem. Mater.*, 2007, **19**, 4379.
- 41 J. C. Park, E. Heo, A. Kim, M. Kim, K. H. Park and H. Song, *J. Phys. Chem. C*, 2011, **115**, 15772.
- 42 L. Tan, X. Wu, D. Chen, H. Liu, X. Meng and F. Tang, *J. Mater. Chem. A*, 2013, **1**, 10382.
- 43 Z. Chen, Z.-M. Cui, F. Niu, L. Jiang and W.-G. Song, *Chem. Commun.*, 2010, **46**, 6524.
- 44 H. Li, B. Xu, X. Liu, A. Sigen, C. He, H. Xia and Y. Mu, *J. Mater. Chem. A*, 2013, **1**, 14108.
- 45 P. Li, P.-P. Huang, F.-F. Wei, Y.-B. Sun, C.-Y. Cao and W.-G. Song, *J. Mater. Chem. A*, 2014, **2**, 12739.
- 46 J. Gascon, U. Aktay, M. D. Hernandez-Alonso, G. P. M. van Klink and F. Kapteijn, *J. Catal.*, 2009, **261**, 75.
- 47 J.-H. Li, W.-J. Liu and Y.-X. Xie, *J. Org. Chem.*, 2005, **70**, 5409.
- 48 A. Indra, C. S. Gopinath, S. Bhaduri and G. K. Lahiri, *Catal. Sci. Technol.*, 2013, **3**, 1625.
- 49 V. I. Nefedov, Y. V. Salyn, G. Leonhardt and R. Scheibe, *J. Electron Spectrosc. Relat. Phenom.*, 1977, **10**, 121.
- 50 K. Nakamoto, in *Infrared and Raman Spectra of Inorganic and Coordination Compounds Part B*, Wiley, New Jersey, 6th edn, 2009, pp. 10–11.
- 51 P. Brant, L. S. Benner and A. L. Balch, *Inorg. Chem.*, 1979, **18**, 3422.
- 52 J. M. Tura, P. Regull, L. Victori and M. Dolors de Castellar, *Surf. Interface Anal.*, 1988, **11**, 447.
- 53 K. Shimizu, R. Maruyama, S. Komai, T. Kodama and Y. Kitayama, *J. Catal.*, 2004, **227**, 202.
- 54 K. Mori, K. Yamaguchi, T. Hara, T. Mizugaki, K. Ebitani and K. Kaneda, *J. Am. Chem. Soc.*, 2002, **124**, 11572.
- 55 N. T. S. Phan, M. V. D. Sluys and C. W. Jones, *Adv. Synth. Catal.*, 2006, **348**, 609.
- 56 J. M. Richardson and C. W. Jones, *Adv. Synth. Catal.*, 2006, **348**, 1207.
- 57 J. M. Richardson and C. W. Jones, *J. Catal.*, 2007, **251**, 80.
- 58 S. Bhunia, R. Sen and S. Koner, *Inorg. Chim. Acta*, 2010, **363**, 3993.
- 59 D. Sengupta, J. Saha, G. De and B. Basu, *J. Mater. Chem. A*, 2014, **2**, 3986.
- 60 A. Fihri, M. Bouhrara, B. Nekouishahraki, J.-M. Basset and V. Polshettiwar, *Chem. Soc. Rev.*, 2011, **40**, 5181.
- 61 I. W. Davies, L. Matty, D. L. Hughes and P. J. Reider, *J. Am. Chem. Soc.*, 2001, **123**, 10139.